Строительные материалы и изделия
Construction Materials and Products

journal homepage: https://bstu-journals.ru

ISSN
2618-7183

DOI: 10.58224/2618-7183-2023-6-6-7

Failure criterion for concrete under volumetric stress state conditions

Agapov V.P. [1], **Markovich A.S.*** [1,2]

[1] RUDN University, Russia,
[2] National Research Moscow State University of Civil Engineering, Russia.

Abstract. Based on the experiments conducted by the authors, a six-parameter failure criterion for concrete has been developed, which makes it possible to take into account the volumetric stress state in strength calculations of massive concrete and reinforced concrete structures. The developed strength criterion is adapted to a spatial eight-node finite element (solid type) and implemented in the PRINS software. To verify the developed criterion, the work provides a com-parison with both experimental data and calculation results that meet other strength criteria widely used for concrete. Thus, the compression and tension meridians of the developed fracture criterion were compared with experimental data, as well as with the Willam & Warnke criterion and the modified Drucker & Prager criterion with Mohr & Coulomb constants. A comparison of compression meridians shows that in the mode of low hydrostatic stresses $\left(\sigma_{okT}/R_b<1\right)$, these criteria converge with each other and with experimental data.
In the mode of average hydrostatic stresses $\left(1\le\sigma_{okT}/R_b\le 2\right)$, the criterion proposed by the authors and the Willam & Warnke criterion show similar results, while the modified Drucker & Prager criterion shows on 20% overestimation of the failure value.
In the mode of high hydrostatic stresses $\left(2\le\sigma_{okT}/R_b\le 3{,}5\right)$, the Willam & Warnke criterion in comparison with the proposed criterion and experimental data, gives an underestimated value of concrete failure.
Keywords: failure criterion for concrete, Drucker & Prager criterion, Willam & Warnke criterion, finite element method, PRINS software, building structures, massive reinforced concrete structures, physical nonlinearity, mechanics of deformable bodies

Please cite this article as: Agapov V.P., Markovich A.S. Failure criterion for concrete under volumetric stress state conditions. Construction Materials and Products. 2023. 6 (6). 7. DOI: 10.58224/2618-7183-2023-6-6-7

*Corresponding author E-mail: markovich-as@rudn.ru

Received August 10, 2023; Received in revised form October 20, 2023; Accepted November 22, 2023

1. INTRODUCTION

Strength calculations of concrete and reinforced concrete structures should be made taking into account the volumetric stress state using numerical methods, in particular, the finite element method [1, 2]. When constructing finite element models, reliable, experimentally verified failure criterion must be used.

According to the authors of this article, it is impossible to obtain a reliable concrete failure criterion in a purely theoretical way. Therefore, to develop such a criterion, it is necessary to use experimental and theoretical methods.

The problem of phenomenological theories of concrete strength and their analysis is carried out in [3-5].

To solve this problem, this article presents a methodology for experimental research aimed at determining the strength of concrete under volumetric stress conditions.

A large number of works by both foreign [6-8] and russian [9-11] researchers are devoted to the study of the strength and deformation of concrete and reinforced concrete elements under the influence of a triaxial stress state.

However, reliable testing of concrete for uneven triaxial compression is quite expensive. To carry them out, it is necessary to manufacture a special testing machine that can provide the required lateral compression of concrete speci-mens in different modes [12].

Due to limited material and technical resources, the authors of this article con-ducted triaxial tests of concrete under conditions of uniform lateral compression of concrete specimens.

Thus, for the experiments, a series of specimens were made, the concrete body of which was enclosed in a steel cage.

To regulate the amount of lateral compression of concrete, steel cages of vari-ous diameters with different heights and wall thicknesses were used.

Based on the results of the experiments, a six-parameter concrete failure criterion was developed, adapted to an eight-node finite element (solid type).

The proposed failure criterion and the corresponding surface in the space of principal stresses can be considered as a failure surface in the case of a model of brittle fracture of concrete in a compressed area, and also interpreted as a limiting yield surface in the case of a model of concrete as an elasto-plastic material.

The specified finite element is implemented in the PRINS software.

2. METHODS AND MATERIALS

Testing concrete for uneven triaxial compression

For the experiments, cages with a diameter of 114, 127, 150, 159 mm and a height of 90, 140, 250, 288 mm were used. A total of 19 specimens were manufactured.

The average value of concrete strength for uniaxial compression was deter-mined on cylinder specimens with a diameter of 150 mm and a height of 300 mm amounted to $R_b = 57$ MPa.

To study the stress-strain state of the specimens, strain gauges BX 120-5AA with a resistance of 120 Ohms were glued to the steel cage.

The experiments were carried out on the Matest testing machine (Fig. 1).

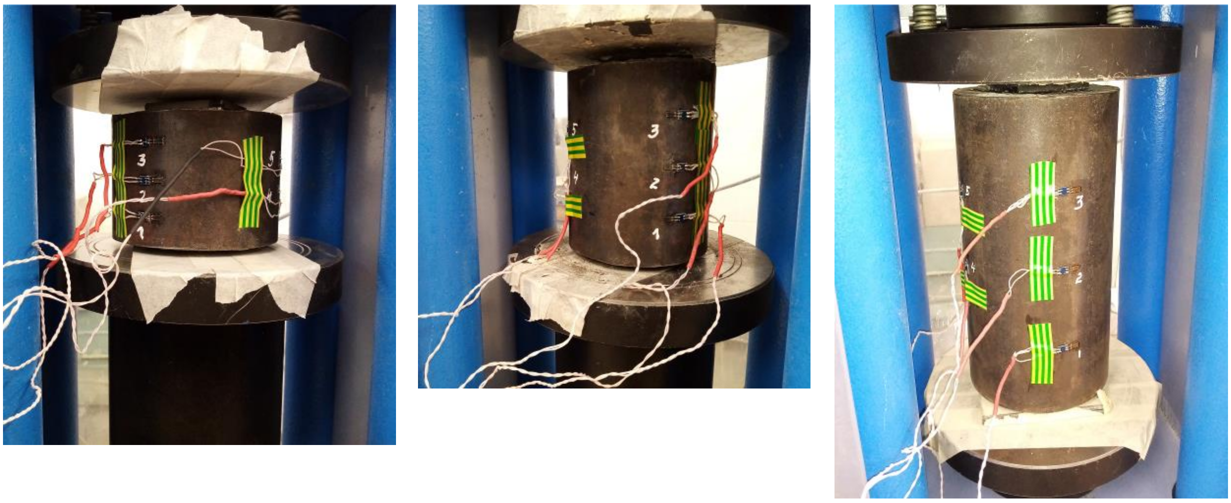

Fig. 1. General view of the specimens.

During the experiments, the load applied to the specimens and the deformations of the steel cage were recorded synchronously, which made it possible to analyze the stress-strain state of each specimens.

The tests were carried out with a constant loading rate of 2 kN/s. The failure of the specimens was a drop in the applied load to 60% of the peak value.

The normalized strength of concrete based on test results, expressed in terms of stresses on the octahedral areas σ_{okT}/R_b and τ_{okT}/R_b is given in Table 1.

Table 1. Experimental results.

Number	Specimens name	Normalized strength	
		σ_{okT}/R_b	τ_{okT}/R_b
1	C16.9-3	0.953	1.025
2	C13.9-3	1.169	1.249
3	C11.9-3	1.429	1.571
4	C16.9-4	1.293	1.398
5	C13.9-4	1.588	1.709
6	C11.9-4	1.953	2.162
7	C16.14-3	1.068	1.187
8	C13.14-3	1.160	1.235
9	C11.14-3	1.251	1.318
10	C16.14-4	1.445	1.613
11	C13.14-4	1.533	1.628
12	C11.14-4	1.653	1.738
13	C16.25-3	1.132	1.278
14	C13.25-3	1.160	1.237
15	C11.25-3	1.274	1.351
16	C16.25-4	1.613	1.850
17	C13.25-4	1.533	1.628
18	C11.25-4	1.720	1.832
19	C15.28-4	1.273	1.380

The form of destruction of the specimens (Fig. 2) indicates that under conditions of uneven triaxial compression, concrete is characterized by pronounced plastic deformation. This circumstance is observed at average (hydrostatic) stress values of $\sigma_0 > 2R_b$. Researchers came to similar conclusions in articles [13].

Fig. 2. Specimen failure form.

Geometric interpretation of the stress state at a point

Let us consider the deviatoric section of a certain fracture surface Ω. The central axis of this surface coincides with the hydrostatic axis d. Let us assume that the principal stresses σ_1, σ_2, σ_3 are found at a point on a solid body and their directions are determined. Let's choose these directions as coordinate axes, as shown in Fig. 3.

The stress state at point can be represented by the vector $\mathbf{OP}$, the components of which are the principal stresses σ_1, σ_2 and σ_3. Let us decompose this vector into two components: vector $\mathbf{ON}$, directed along the hydrostatic axis d and vector $\mathbf{NP}$, lying in the deviatoric plane.

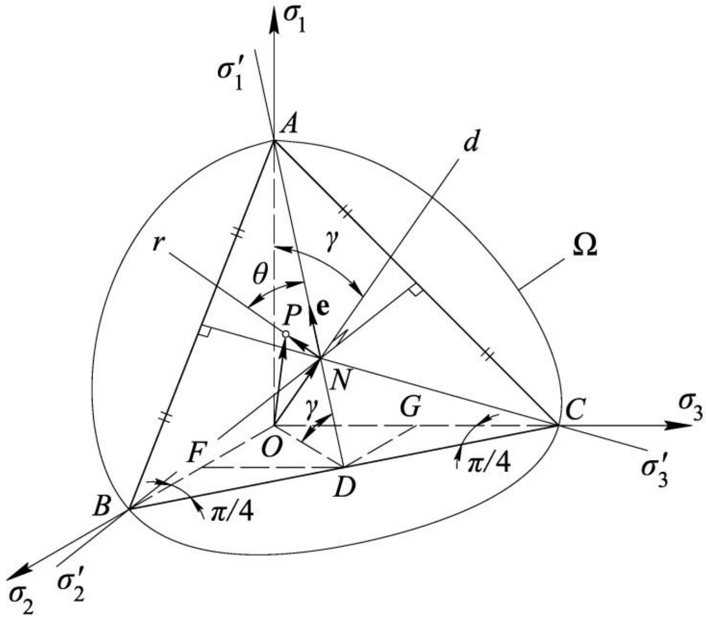

Fig. 3. Geometric interpretation of the stress state at a point.

Therefore, the vectors $\mathbf{ON}$ and $\mathbf{NP}$ have coordinates:

$$\mathbf{ON} = \sigma_0 \left(\mathbf{i}_1 + \mathbf{i}_2 + \mathbf{i}_3 \right), \quad \mathbf{NP} = s_1 \mathbf{i}_1 + s_2 \mathbf{i}_2 + s_3 \mathbf{i}_3, \tag{1}$$

where $\mathbf{i}_1$, $\mathbf{i}_2$, $\mathbf{i}_3$, and are unit vectors of the coordinate axes σ_1, σ_2 and σ_3 respectively.

The lengths of the $|\mathbf{ON}| = \xi$ and $|\mathbf{NP}| = r$ vectors are determined from the following relations:

$$\xi = \frac{1}{\sqrt{3}} I_1 \left(T_\sigma \right) = \sqrt{3} \sigma_{okT}, \quad r = \sqrt{2 I_2 \left(D_\sigma \right)} = \sqrt{3} \tau_{okT}, \tag{2}$$

where σ_{okT} and τ_{okT} are normal and shear stresses on the octahedral areas, $I_1(T_\sigma)$ and $I_2(D_\sigma)$ are the first invariant of the stress tensor and the second invariant of the stress deviator.

Thus, the vector **ON** determines the hydrostatic component (ξ), and **NP** – the deviatoric component (r) of the total stress state at point P.

The angle of the stress state θ is found from the condition:

$$\cos\theta = \frac{1}{r}(\mathbf{NP}\cdot\mathbf{e}). \tag{3}$$

Whence

$$\cos\theta = \frac{2\sigma_1 - \sigma_2 - \sigma_3}{\sqrt{2(\sigma_1-\sigma_2)^2 + 2(\sigma_2-\sigma_3)^2 + 2(\sigma_3-\sigma_1)^2}}, \tag{4}$$

or

$$\cos 3\theta = \frac{3\sqrt{3}}{2}\frac{I_3(D_\sigma)}{\sqrt{\left[I_2(D_\sigma)\right]^3}} = \frac{\sqrt{2}}{\tau_{okT}^3} I_3(D_\sigma), \tag{5}$$

where $I_3(D_\sigma)$ is the third invariant of the stress deviator.

The derivation of formulas (2), (4) and (5) is given in the monograph [14].

3. RESULTS AND DISCUSSION

Relations for the fracture surface curve in the deviatoric plane

If consider concrete as an isotropic material, then its fracture surface in the space of principal stresses $\sigma_1 - \sigma_2 - \sigma_3$ will be a surface of rotation symmetrical relative to the hydrostatic axis (Fig. 4, a).

In Fig. 4, b shows the deviatoric section of such a fracture surface. Since this section has triple symmetry, it is enough to know the equation of the curve within the $0 < \theta < \pi/3$ – sector. For this, we use polar coordinates, as shown in Fig. 4, *b*.

To represent the deviatoric section curves of the fracture surface, the approach of Willam & Warnke [15] was used.

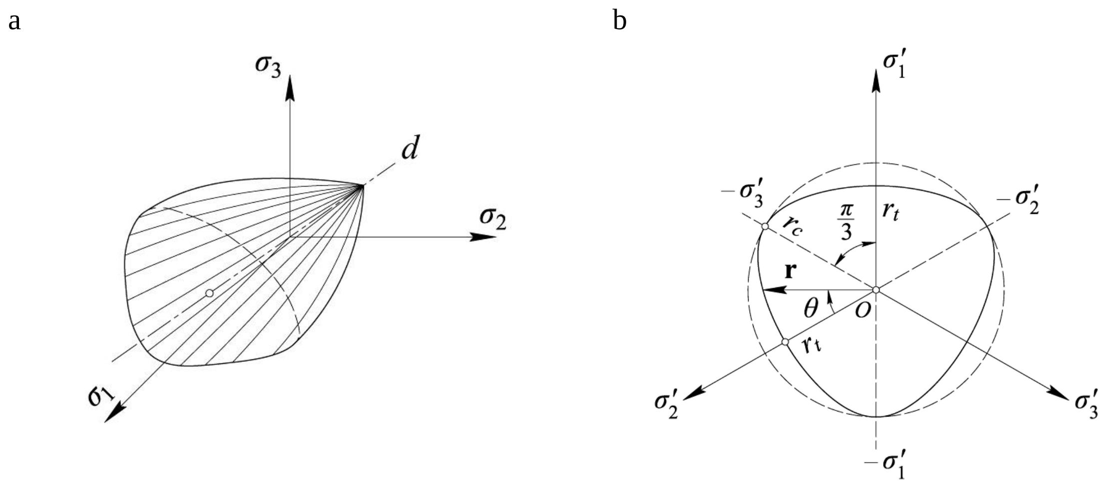

Fig. 4. Concrete fracture surface: *a* – general view in the coordinate system $\sigma_1 - \sigma_2 - \sigma_3$; *b* – deviatoric section.

The equation of an elliptic curve within the specified sector with semi-axes a and b (Fig. 5) has the form:

$$f(x,y)=\frac{x^2}{a^2}+\frac{y^2}{b^2}-1=0. \tag{6}$$

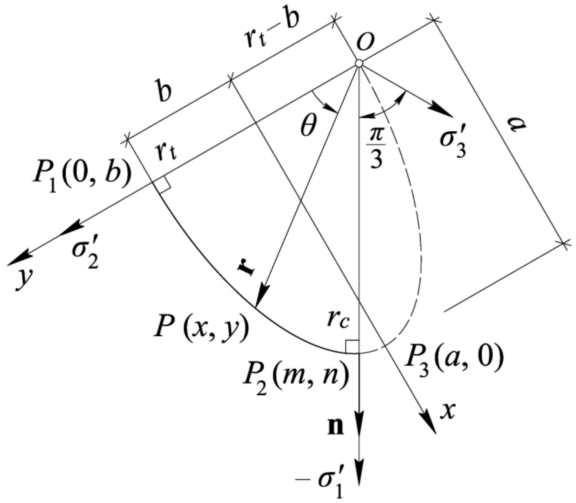

Fig. 5. Elliptic curve of concrete failure surface for sector $0<\theta<\pi/3$.

The coordinates of the normal vector to the ellipse at point $P_2(m,n)$ are determined by differentiation (6):

$$\mathbf{n}=\begin{Bmatrix}\dfrac{\partial f/\partial x}{\sqrt{(\partial f/\partial x)^2+(\partial f/\partial y)^2}}\\ \dfrac{\partial f/\partial y}{\sqrt{(\partial f/\partial x)^2+(\partial f/\partial y)^2}}\end{Bmatrix}^T=\left\{\frac{m/a^2}{\sqrt{m^2/a^4+n^2/b^4}}\ ,\ \frac{n/b^2}{\sqrt{m^2/a^4+n^2/b^4}}\right\} \tag{7}$$

The equations for determining the dimensions of the semi-axes of an ellipse are written as follows:

$$a^2=\frac{r_c(r_t-2r_c)^2}{5r_c-4r_t},\qquad b=\frac{2r_t^2-5r_tr_c+2r_c^2}{4r_t-5r_c}. \tag{8}$$

Using the relationship between cartesian and polar coordinates, we obtain that

$$x=r(\theta)\sin\theta,\qquad y=r(\theta)\cos\theta-(r_t-b). \tag{9}$$

Substituting into equation (6), we get:

$$\frac{\left[r(\theta)\sin\theta\right]^2}{a^2}+\frac{\left[r(\theta)\cos\theta-(r_t-b)\right]^2}{b^2}=1. \tag{10}$$

By making simple mathematical operations, the length of the radius vector $\mathbf{r}$ within the $0<\theta<\pi/3$ – sector can be determined by the formula:

$$r(\theta)=\frac{2r_c\left(r_c^2-r_t^2\right)\cos\theta+r_c\left(2r_t-r_c\right)\sqrt{4\left(r_c^2-r_t^2\right)\cos^2\theta+5r_t^2-4r_tr_c}}{4\left(r_c^2-r_t^2\right)\cos^2\theta+\left(r_c-2r_t\right)^2}\,. \tag{11}$$

It is obvious that at $r_t=r_c$ the deviatoric section will be a circle, and the fracture surface will degenerate into a conical surface symmetrical relative to the hydrostatic axis.

Relations for the compression and tension meridians of the fracture surface

For the meridional curves of the fracture surface, an equation is adopted that relates normal and shear stresses on octahedral areas:

$$f(\boldsymbol{\sigma})=f\left(\sigma_{okT},\tau_{okT},\theta\right)=\frac{1}{r\left(\sigma_{okT},\theta\right)}\frac{\tau_{okT}}{R_b}-1=0\,. \tag{12}$$

In this case, the tensile $(\theta=0)$ and compression $(\theta=\pi/3)$ meridians of the fracture surface are described by quadratic functions:

$$\left(\frac{\tau_{okT}}{R_b}\right)_t=\frac{r_t}{R_b\sqrt{3}}=A_0+A_1\frac{\sigma_{okT}}{R_b}+A_2\left(\frac{\sigma_{okT}}{R_b}\right)^2,\quad \text{at } \theta=0\,, \tag{13}$$

$$\left(\frac{\tau_{okT}}{R_b}\right)_c=\frac{r_c}{R_b\sqrt{3}}=B_0+B_1\frac{\sigma_{okT}}{R_b}+B_2\left(\frac{\sigma_{okT}}{R_b}\right)^2,\quad \text{at } \theta=\pi/3\,, \tag{14}$$

where A_0, A_1, A_2 and B_0, B_1, B_2 are the criterion parameters.

To determine the criterion parameters A_0, A_1, A_2 and B_0, B_1, B_2 for a specific class of concrete, it is necessary to conduct five standard tests (Table 2).

Table 2. Concrete testing.

Standard concrete test	σ_{okT}/R_b	τ_{okT}/R_b	Angle θ
1. Uniaxial compression, $\sigma_3=-R_b$, $\sigma_1=\sigma_2=0$	$-\frac{1}{3}$	$\frac{\sqrt{2}}{3}$	$\pi/3$
2. Uniaxial tension, $\sigma_1=R_{bt}$, $\sigma_2=\sigma_3=0$, $\bar{R}_{bt}=1/12$	$\frac{1}{3}\bar{R}_{bt}$	$\frac{\sqrt{2}}{3}\bar{R}_{bt}$	0
3. Uniform biaxial compression, $\sigma_2=\sigma_3=-R_{bc}$, $\sigma_1=0$, $\bar{R}_{bc}=1{,}4$*	$-\frac{2}{3}\bar{R}_{bc}$	$\frac{\sqrt{2}}{3}\bar{R}_{bc}$	0
4. Uniform triaxial tension $(\sigma_1=\sigma_2=\sigma_3=R_{bt})$, $\sigma_1\neq0$, $\sigma_2\neq0$, $\sigma_3\neq0$	$\sigma_{okT}/R_b=\bar{\xi}_0$, $\bar{\xi}_0>0$	0	0, $\pi/3$
5. Triaxial compression in low compression mode $(\sigma_3>\sigma_1=\sigma_2,\ \theta=\pi/3)$	$\sigma_{okT}/R_b=-\bar{\xi}_c$, $\bar{\xi}_c>0$, $\tau_{okT}/R_b=\bar{r}_c$	$\sigma_1\neq0$, $\sigma_2\neq0$, $\sigma_3\neq0$, $\bar{\xi}_c=1{,}273$**, $\bar{r}_c=1{,}380$**	$\pi/3$

* *According to the results of tests Telichko V.G. & Ziborova L.A. [16]*

** *According to the authors' test results*

On the tension meridian $(\theta = 0)$ there are points of uniaxial tension (R_{bt}) and uniform biaxial compression (R_{bc}) and on the compression meridian $(\theta = \pi/3)$ there are points of uniaxial (R_b) and uneven triaxial compression in the low lateral pressure mode $(\sigma_3 > \sigma_1 = \sigma_2)$. In this case, the top of the fracture surface corresponds to the point of uniform triaxial tension $(\sigma_1 = \sigma_2 = \sigma_3)$.

Using concrete test results (table 2), each of equations (13) and (14) forms a system of three independent equations.

So, for the tension meridian $(\theta = 0)$:

$$\frac{\sqrt{2}}{3}\bar{R}_{bt} = A_1 - \frac{1}{3}A_2\bar{R}_{bt} + \frac{1}{9}A_3\bar{R}_{bt}^2, \quad \frac{\sqrt{2}}{3}\bar{R}_{bc} = A_1 + \frac{2}{3}A_2\bar{R}_{bc} + \frac{4}{9}A_3\bar{R}_{bc}^2,$$
$$0 = A_1 - A_2\bar{\xi}_0 + A_3\bar{\xi}_0^2. \tag{15}$$

For the compression meridian $(\theta = \pi/3)$:

$$\frac{\sqrt{2}}{3} = B_1 + \frac{1}{3}B_2 + \frac{1}{9}B_3, \quad \bar{r}_c = B_1 + B_2\bar{\xi}_c + B_3\bar{\xi}_c^2,$$
$$0 = B_1 - B_2\bar{\xi}_0 + B_3\bar{\xi}_0{}^2. \tag{16}$$

Solving equations (15) and (16) relative to A_0, A_1, A_2 and B_0, B_1, B_2, we obtain the required criterion parameters:

$$A_1 = A_2\bar{\xi}_0 - A_3\bar{\xi}_0^2, \quad A_2 = \frac{\frac{\sqrt{2}}{3}\bar{R}_{bt} - A_3\left(\frac{1}{9}\bar{R}_{bt}^2 - \bar{\xi}_0^2\right)}{\bar{\xi}_0 - \frac{1}{3}\bar{R}_{bt}},$$
$$A_3 = \frac{\frac{\sqrt{2}}{3}\left(\bar{R}_{bc} - \bar{R}_{bt}\dfrac{\bar{\xi}_0 + \frac{2}{3}\bar{R}_{bc}}{\bar{\xi}_0 - \frac{1}{3}\bar{R}_{bt}}\right)}{\frac{4}{9}\bar{R}_{bc}^2 - \bar{\xi}_t^2 - \left(\frac{1}{9}\bar{R}_{bt}^2 - \bar{\xi}_t^2\right)\dfrac{\bar{\xi}_0 + \frac{2}{3}\bar{R}_{bc}}{\bar{\xi}_0 - \frac{1}{3}\bar{R}_{bt}}} \tag{19}$$

and

$$B_1 = B_2\bar{\xi}_0 - B_3\bar{\xi}_0{}^2, \quad B_2 = \frac{\bar{r}_c - B_3\left(\bar{\xi}_c^2 - \xi_0{}^2\right)}{\bar{\xi}_0 + \bar{\xi}_c},$$
$$B_3 = \frac{\bar{r}_c\left(3\bar{\xi}_0 + 1\right) - \sqrt{2}\left(\bar{\xi}_0 + \bar{\xi}_c\right)}{3\left(\bar{\xi}_c^2 - \bar{\xi}_0{}^2\right)\left(\bar{\xi}_0 + \frac{1}{3}\right) + 3\left(\bar{\xi}_0 + \bar{\xi}_c\right)\left(\bar{\xi}_0{}^2 - \frac{1}{9}\right)}. \tag{20}$$

For an arbitrary angle of stress state θ, the deviatoric coordinate $r(\theta)$ is determined by formula (11) depending on the values of $r_t = \sqrt{3}\bar{r}_t R_b$ and $r_c = \sqrt{3}\bar{r}_c R_b$. In its turn, the coordinate $\xi = \sqrt{3}\bar{\xi} R_b$.

In Fig. 6 and Fig. 7 shows a comparison of the compression $(\theta = \pi/3)$ and tension $(\theta = 0)$ meridians of this fracture criterion with experimental data [17-18], as well as with the Willam & Warnke criterion [15] and the modified Drucker & Prager criterion with Mohr – Coulomb constants.

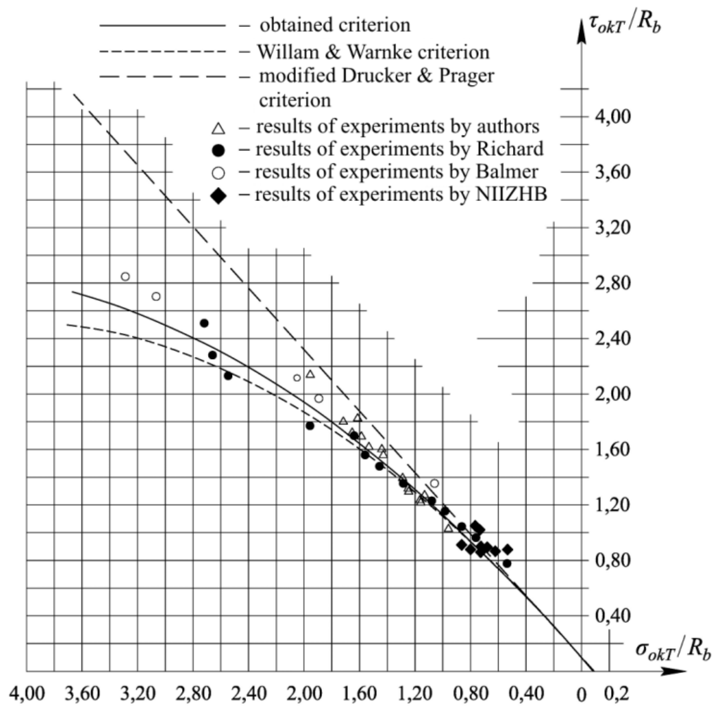

Fig. 6. Comparison of the compression meridian $(\theta = \pi/3)$ of this criterion with experimental data and the Willam & Warnke, Drucker & Prager criteria.

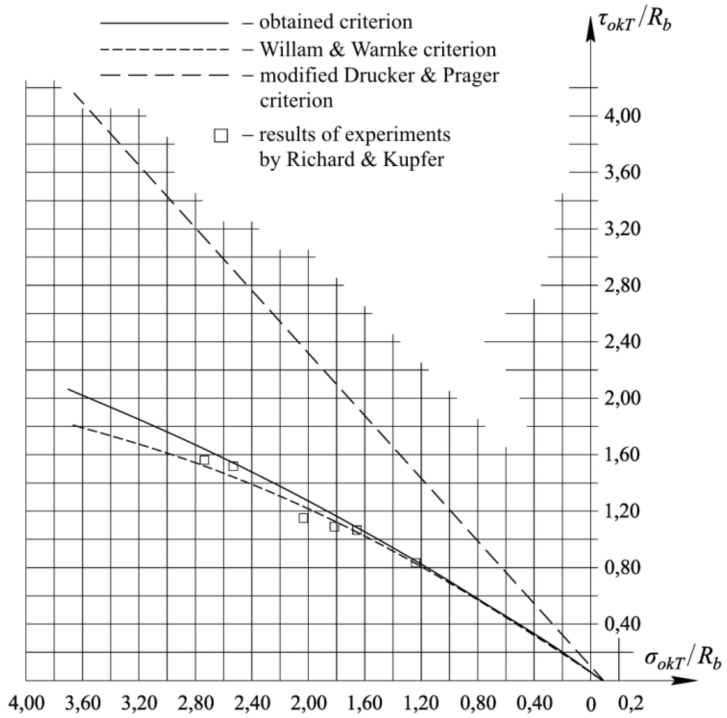

Fig. 7. Comparison of the tension meridian $(\theta = 0)$ of this criterion with experimental data and Willam & Warnke, Drucker & Prager criteria.

The following material parameters were used in the Willam & Warnke criterion [15]: $\bar{R}_{bt} = 1/12$, $\bar{R}_{bc} = 1{,}4$, $(\sigma_0/R_b)_c = -3{,}67$, $(\tau_0/R_b)_c = 2{,}5$ and $(\sigma_0/R_b)_t = -3{,}67$, $(\tau_0/R_b)_t = 2{,}05$.

The modified Drucker & Prager criterion, expressed in terms of stresses on the octahedral areas, is written as:

$$\bar{r}(\bar{\xi}) = \frac{\sqrt{2}k - \sqrt{6}\alpha\bar{\xi}\sqrt{3}R_b}{\sqrt{3}R_b}, \tag{21}$$

where $\bar{\xi} = \dfrac{\sigma_{okT}}{R_b}$ and $\bar{r} = \dfrac{\tau_{okT}}{R_b}$.

The parameters of the Drucker & Prager criterion associated with the Mohr –Coulomb constants (cohesion c and angle of internal friction φ) are determined by the equations:

$$\alpha = \frac{2\sin\varphi}{\sqrt{3}(3-\sin\varphi)}, \quad k = \frac{6c\cos\varphi}{\sqrt{3}(3-\sin\varphi)}, \quad \bar{\xi}_0 = \frac{k}{3\alpha R_b}. \tag{22}$$

In its turn, the Mohr – Coulomb constants for concrete are determined from the conditions:

$$\sin\varphi = \frac{m-1}{m+1}, \quad c = \frac{R_b(1-\sin\varphi)}{2\cos\varphi}, \quad m = \frac{1}{\bar{R}_{bt}}. \tag{23}$$

4. CONCLUSIONS

A comparison of compression meridians $(\theta = \pi/3)$ shows that in the mode of low hydrostatic stresses $(\sigma_{okT}/R_b < 1)$, these criteria converge with each other and with experimental data. In the mode of average hydrostatic stresses $(1 \le \sigma_{okT}/R_b \le 2)$, the criterion proposed by the authors and the Willam & Warnke criterion show similar results, while the modified Drucker & Prager criterion shows on 20% overestimation of the failure value.

In the mode of high hydrostatic stresses $(2 \le \sigma_{okT}/R_b \le 3{,}5)$, the Willam & Warnke criterion in comparison with the proposed criterion and experimental data, gives an underestimated value of concrete failure.

It is worth noting that for $\sigma_{okT}/R_b > 2{,}5$ there is a significant scatter in the experimental data, and for $\sigma_{okT}/R_b >> 3$ the strength of concrete has not been sufficiently researched experimentally.

Reliable experimental data on the tension meridian $(\theta = 0)$ are limited [19-21]. As can be seen from Fig. 7 in the mode $3 \ge \sigma_{okT}/R_b \ge 1$, the strength of concrete according to the proposed criterion and the Willam & Warnke criterion corresponds to experimental data

At the tensile meridian $(\theta = 0)$, the Drucker & Prager criterion shows an erroneously overestimated value of concrete failure. This is explained that the Drucker & Prager criterion in the space of principal stresses represents a conical surface of rotation with straight meridians, symmetrical relatively to the hydrostatic axis, which is equivalent to $R_{bt} = R_b$.

The accepted mathematical representation of the specified failure criteria is due to the convenience of software implementation by the finite element method.

Thus, the proposed failure criterion and the corresponding surface in the space of principal stresses can be considered as a failure surface in the case of a model of brittle fracture of concrete in a compressed area, and also interpreted as a limiting yield surface in the case of a model of concrete as an elastoplastic material.

The given failure criterion of concrete was implemented in the PRINS software [14]. It allows to perform calculations of concrete and reinforced concrete structures according to the volumetric stress state, using the finite element method in a physically nonlinear formulation.

REFERENCES

[1] Agapov V.P. Finite element method in statics, dynamics and stability of structures. publishing house ASV. 2005. 245 p.

[2] Zienkiewicz O.C., Taylor R.L. The finite element method for solid and structural mechanics. Sixth edition. McGraw-Hill. 2005. 631 p.

[3] Mohammed J. Alttaee, Majid M.A. Kadhim, Sarmed S. Altayee, Ali H. Adheem. Employment of damage plasticity constitutive model for concrete members subjected to high strain-rate. Proceedings of the 1st International Multi-Disciplinary Conference Theme: Sistainable Development and Smart Planning. IMDC-SDSP 2020. June 2020. DOI: 10.4108/eai.28-6-2020.2298164

[4] Hu L., Li S., Zhu J., Yang X. Mathematical model of constitutive relation and failure criteria of plastic concrete under true triaxial compressive stress. Materials. 2021. 14 (1). 102. https://doi.org/10.3390/ma14010102

[5] Korsun V.I., Nedorezov A.V., Makarenko S.Yu. Comparative analysis of strength criteria for concrete. Modern Industrial and Civil Construction. 2014. 10 (1) P. 65 – 78. URL: https://www.researchgate.net/publication/310255312_Sopostavitelnyj_analiz_kriteriev_procnosti_dla_betonov

[6] Zhenpeng Yu, Qiao Huang, Furong Li, Yue Qin, Jun Znang. Experimental study on mechanical properties and failure criteria of self-compacting concrete under biaxial tension-compression. Journal of Materials in Civil Engineering. 2019. 31. 10.1061/(ASCE)MT.1943-5533.0002675

[7] Tan T.H. Effects of triaxial stress on concrete. 30th Conference on our world in concrete and structures. CI Premier Pte Ltd. Singapore: CI Premier Pte Ltd. 2005. 10 p. URL: http://www.cipremier.com/e107_files/downloads/Papers/ 100/30/100030007.pdf

[8] Wang H.L, Song Y.P. Behavior of mass concrete under biaxial compression-tension and triaxial compression-compression-tension. Mater. Struct. 2009. 42. P. 241 – 249. doi:10.1617/s11527-008-9381-y

[9] Karpenko N.I., Eryshev V.A., Latysheva, E.V. Stress-strain diagrams of concrete under repeated loads with compressive stresses. Procedia Engineering. 2015. 111. P. 371 – 377. DOI:10.1016/j.proeng.2015.07.103

[10] Karpenko N.I., Karpenko S.N. About diagram method for construction of the physical proportions for concrete and reinforced concrete elements under volumetric (triaxial) stress state. Textile Industry Technology. 2016. 4 (364). P. 28 – 34.

[11] Karpenko N.I., Karpenko S.I. To determine the strength of concrete under triaxial compress. Concrete Technologies. 2014. 10 (99). P. 40 – 41.

[12] Wang J., Xie F., Zhang C., Ruan J. Experimental study and failure criterion analysis on combined compression-shear performance of self-compacting concrete. Materials. 2020. 13 (3). P. 713. DOI: 10.3390/ma13030713

[13] Thomas Gabet, Malecot Yann, Daudeville Laurent. Ultimate strength of plain concrete under extreme combined stresses. Revue Européenne de Génie Civil. 2006. 10. P. 375 – 389. DOI: 10.1080/17747120.2006.9692834

[14] Agapov V.P., Markovich A.S. Nonlinear models of concrete and reinforced concrete structures. Theory and implementation in VK PRINCE. Mocsow. RUDN. 2023. 264 p.

[15] Willam K.J., Warnke E.P. Constitutive model for the triaxial behavior of concrete. Proceedings of IABSE. Structural Engineering Report 19. Section III. 1975. P. 1 – 30.

[16] Telichko V.G., Ziborov L.A. Strength study under biaxial compression of concrete of class B-25. Izvestiya Tula State University. 2009. P. 89 – 94.

[17] Chen W.F. Plasticity in Reinforced Concrete. J. Ross Publishing. Softcover. 2007. 474 p.

[18] Bofang Zhu. The finite element method: fundamentals and applications in civil, hydraulic, mechanical and aeronautical engineering. John Wiley & Sons Singapore Pte. Ltd. 2018. 872 p.

[19] Zhou Y., Liu X., Xing F., Cui H., Sui L. Axial compressive behavior of FRP-confined lightweight aggregate concrete: an experimental study and stress-strain relation model. Construction and Building Materials. 2016. 119. P. 1 – 15. DOI: 10.1016/j.conbuildmat.2016.02.180
[20] Gabet T., Malecot Y., Daudeville L. Ultimate strength of plain concrete under extreme combined stresses. Revue Européenne de Génie Civil. 2006. 10. P. 375 – 389. DOI:10.1080/17747120.2006.9692834
[21] Shi L., Wang L., Song Y., Shen, L. Dynamic multiaxial strength and failure criterion of dam concrete. Construction and Building Materials. 2014. 66. P. 181 – 191. DOI: 10.1016/j.conbuildmat.2014.05.076

INFORMATION ABOUT THE AUTHORS

Agapov V.P., e-mail: agapovpb@mail.ru, tel.:8(495) 955-09-48, ORCID ID: 0000-0002-1749-5797, SCOPUS: https://www.scopus.com/authid/detail.uri?authorId=57197812573, RUDN University, Engineering academy, Doctor of Technical Sciences, Professor

Markovich A.S., e-mail: markovich-as@rudn.ru, tel.:8(495) 955-09-48, ORCID ID: 0000-0003-3967-2114, SCOPUS: https://www.scopus.com/authid/detail.uri?authorId=57209575592, RUDN University, Engineering academy, National Research Moscow State University of Civil Engineering, Department of Fundamental Education, Candidate of Engineering Sciences (Ph.D.), Associate Professor